Stress intensity factor solution for edge interface crack based on the crack tip stress without the crack

Stress intensity factor solution for edge interface crack based on the crack tip stress without the crack

Kazuhiro ODA[a]*, Yosuke TAKAHATA[b], Yuya KASAMURA[b], and Nao-Aki NODA[c]*
* Corresponding authors
[a] Division of Mechanical Engineering, Faculty of Science and Technology, Oita University, 700 Dannoharu, Oita-shi, Oita 870-1192, Japan
E-mail: oda-kazuhiro@oita-u.ac.jp
[b] Mechanical and Energy Systems Engineering Course, Graduate School of Oita University, 700 Dannoharu, Oita-shi, Oita 870-1192, Japan
[c] Department of Mechanical Engineering, Kyushu Institute of Technology, 1-1 Sensui-cho, Tobata-ku, Kitakyushu-shi, Fukuoka 804-8550, Japan

Abstract
In this paper, a new solution is discussed for the stress intensity factor of an edge interface crack. The intensity of the singular stress field (ISSF) at the interface end before appearing the edge interface crack is distinguished from the stress intensity factor (SIF) of the interface crack itself. By considering those two distinct double singular stress fields, the ISSF and the SIF are discussed under arbitrary material combinations. By focusing on the crack tip stress without the interface crack $\sigma_y(a)$, the SIF of the edge interface crack can be expressed conveniently. This is because the crack tip stress without the interface crack is reflecting the ISSF at the interface end. The SIFs based on the crack tip stress without the interface crack are indicated by varying the crack length and material combination. It is found that the normalized SIFs ($F_{1,\mathrm{int}}$ and $F_{2,\mathrm{int}}$) based on $\sigma_y(a)$ are independent of the geometrical condition for the wide range of the crack length.

Key words : Stress intensity factor, Intensity of singular stress field, Interface crack, Butt joint, Finite element method

Nomenclature

a	length of the edge interface crack
b, c	half the length of the major and minor axes of an elliptical hole
$C_1(\alpha,\beta)$, $C_2(\alpha,\beta)$	normalized factors for edge interface crack
E	Young's modulus
$F_1(\alpha,\beta)$, $F_2(\alpha,\beta)$	normalized stress intensity factors for edge interface crack based on applied stress
$F_{1,\mathrm{int}}(\alpha,\beta)$, $F_{2,\mathrm{int}}(\alpha,\beta)$	normalized stress intensity factors for edge interface crack based on $\sigma_y(a)$
$F_I(0,0)$	normalized stress intensity factor for edge crack in a homogeneous semi-infinite plate
$f_{r\theta}$, $f_{\theta\theta}$	angular functions
G	shear modulus
h	bond line thickness of sandwiched butt joint plate
K_1, K_2	stress intensity factors of an edge interface crack in a bonded plate
K_I	stress intensity factor of an crack in a homogeneous plate
K_σ	intensity of singular stress field (ISSF)
L	height of the bonded plate
r	distance from the interface end
T_y, S	tensile and shear stresses applied to the reference problem
W	width of the bonded plate
α, β	Dundurs' material composite parameters
ε	oscillation singular index of an interface crack

ρ	radius of curvature of an elliptical hole
σ_0	applied remote stress
σ_y, τ_{xy}	stress components along the bi-material interface
$\sigma_y(a)$	singular stress along the interface at the crack tip point
λ	order of the stress singularity at the interface end
ν	Poisson's ratio

1. Introduction

A number of studies are available regarding interface cracks. Different from ordinary cracks, the interface stress intensity factor SIF varies depending on the material combination as well as the geometries. They are useful for evaluating the interface strength of dissimilar materials [1-6]. Recently, the adhesive strength was discussed in terms of the SIF of the interface crack [7-8]. The butt joint strength can be expressed as a constant value of the intensity of singular stress field (ISSF) at the interface end [9-13]. Also, by assuming a fictitious edge interface crack at the interface end, the butt joint strength also can be expressed as a constant value of the SIF [14,15]. Those interface fracture mechanics approach shows the usefulness of the solution of the edge interface crack.

However, great care should be taken for another singular stress field before appearing the edge interface crack as shown in Fig.1 (b). Since this singular stress field is totally different from the singular stress field due to the interface crack, double singular stress fields must be considered to clarify edge interface crack problems. Those double singular stress fields have not been focused in the previous studies. In this paper, therefore, the intensities of those double singular stress fields are denoted by the ISSF and the SIF and will be discussed independently as shown in Fig.1. Since the small edge interface crack appears within the region of the singular stress field in Fig.1, this approach will clarify the interface crack problem. This is because the SIF for the small edge interface cracks are controlled by the ISSF singular zone at the interface corner for the perfectly bonded strip without crack as shown in Fig. 1.

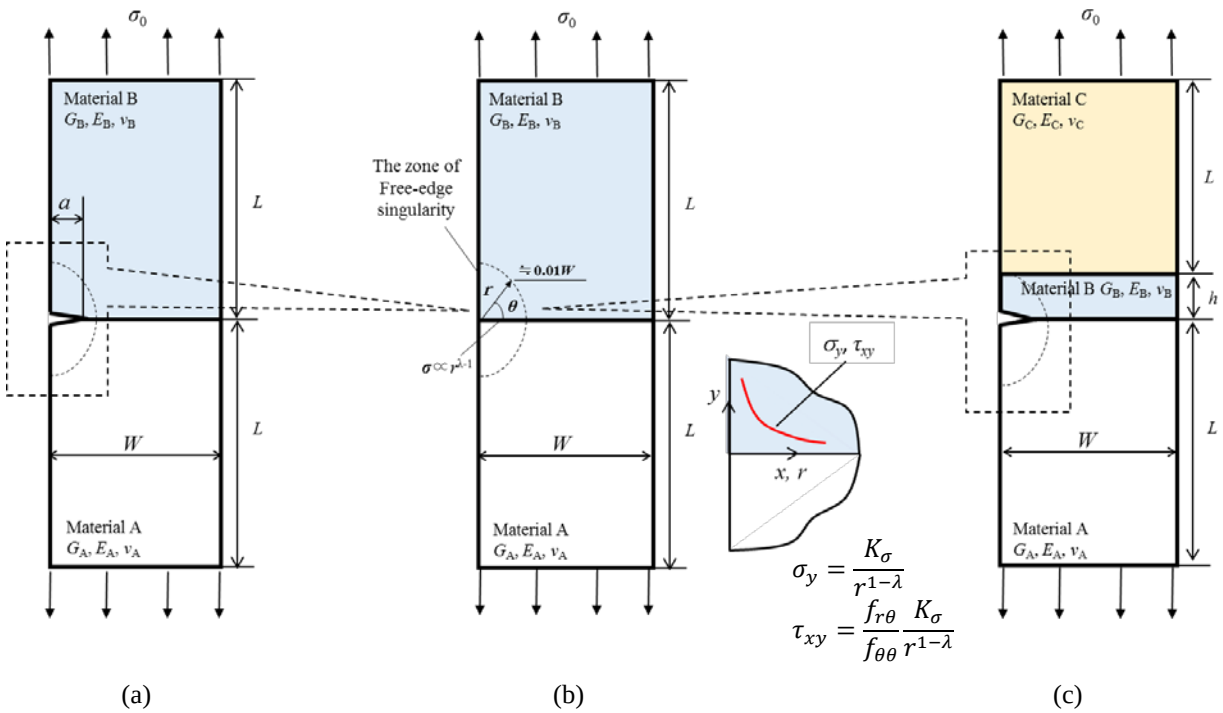

Fig.1 Interface edge crack problems (a) and (c), whose stress intensity factors (SIFs) are controlled by the intensity of the singular stress field (ISSF) of bonded plate problem (b) at the interface end before appearing the interface cracks: (a) Bonded AB plate having an interface crack (b) Bonded AB plate whose singular index is λ before appearing the crack, (c) Bonded ABC plate having an interface crack.

In this paper, therefore, a new solution for the edge interface crack in the bonded AB plate in Fig.1 (a) will be shown by separating the double singular stress fields. Then, the usefulness of the new solution will be shown by applying to the stress intensity factor of a sandwiched ABC plate. Here, bonded AB plate contains two different materials and bonded ABC plate contains three different materials. Then, it will be shown that the new solution for the edge interface crack in the bonded AB plate in Fig.1 (a) can be used conveniently to evaluate the interface crack in bonded ABC plate. In this study, the interfacial crack will be analyzed by applying the finite element method (FEM). The FEM is one of the most used numerical modeling techniques, which can be used for many engineering applications conveniently [24]. To calculate the SIF accurately, the proportional method [16, 17] proposed previously will be applied. The detail will be indicated in Appendix A.

2. Interface crack in bonded plates versus crack in homogeneous plates

2.1 Expression of SIF of Small Edge Interface Crack

Figure 2 shows an edge crack whose length is 'a' in a homogeneous semi-infinite plane under tension σ_0. The stress intensity factor in Fig.2 (a) is known as $K_I = 1.1215\sigma_0\sqrt{\pi a}$. This is equivalent to an internal crack whose crack length is '$2a$' in an infinite plate under internal pressure as shown in Fig.2 (b) and under remote tension $1.1215\sigma_0$ as shown in Fig.2 (c). In Fig.2, one may think why the edge crack geometry is equivalent to a center crack in an infinite plate. The dimensionless stress intensity factor $F_I(0,0)$ can be defined as the stress intensity factor ratio of Fig.2(a) to Fig.2(b). The same stress intensity factor of the center crack as the edge crack can be created by adjusting the internal pressure or by applying the remote tensile stress to the infinite plate having the central crack.

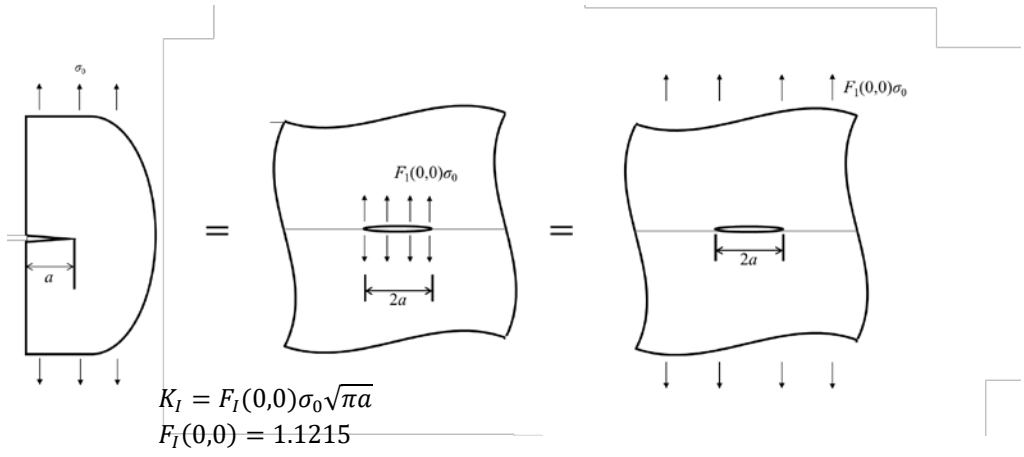

Fig.2 Equivalent crack problems: (a) an edge crack subjected to remote tensile stress, (b) an internal crack subjected to internal pressure and (c) an internal crack in an infinite plate under remote tensile stress

In a similar way, Figure 3 shows equivalent interface cracks in bonded plates. Here, the stress intensity factor of a small edge interface crack in Fig.3 (a) is equivalent to an interface crack subjected to the normal and tangential tractions $F_1(\alpha, \beta)\sigma_0$ and $F_2(\alpha, \beta)\sigma_0$ along the crack surface as shown in Fig.3 (b). The normalized factors $F_1(\alpha, \beta)$ and $F_2(\alpha, \beta)$ are depending on the material combination (α, β) and they varies from 0 to ∞ as shown in Eq. (1). To express the SIF as finite values, $C_1(\alpha,\beta)$, $C_2(\alpha,\beta)$ can be used conveniently [21].

$$K_1 + iK_2 = \{F_1(\alpha,\beta) + iF_2(\alpha,\beta)\}\sigma_0\sqrt{\pi a}(1+2i\varepsilon), \qquad \varepsilon = \frac{1}{2\pi}\ln\left[\left(\frac{\kappa_A}{G_A}+\frac{1}{G_B}\right)\Big/\left(\frac{\kappa_B}{G_B}+\frac{1}{G_A}\right)\right]$$
$$F_1(\alpha,\beta) = 0\sim\infty = C_1(\alpha,\beta)(W/a)^{1-\lambda}, \quad C_1(\alpha,\beta) = finite = 0.46\sim1.24 \tag{1}$$
$$F_2(\alpha,\beta) = 0\sim\infty = C_2(\alpha,\beta)(W/a)^{1-\lambda}, \quad C_2(\alpha,\beta) = finite = -0.379\sim0.031$$

The material combinations (α, β) are Dundurs' composite parameters defined as

$$\alpha = \frac{G_A(\kappa_B + 1) - G_B(\kappa_A + 1)}{G_A(\kappa_B + 1) + G_B(\kappa_A + 1)}, \qquad \beta = \frac{G_A(\kappa_B - 1) - G_B(\kappa_A - 1)}{G_A(\kappa_B + 1) + G_B(\kappa_A + 1)} \tag{2}$$

In Eqs. (1) and (2), the subscript means the material A or B, $G_i=E_i/2(1+\nu_i)$ and the notation ε denotes the oscillation singular index, $\kappa_i = 3-4\nu_i$ for plane strain, $(3-\nu_i)/(1+\nu_i)$ for plane stress. E_i, G_i and ν_i denote Young's modulus, the shear modulus and Poisson's ratio for material i, respectively.

The definition of oscillation stress intensity factor of interface crack is based on the interface crack length $2a$ [3, 5].

$$\sigma_y + i\tau_{xy} = \frac{K_1 + iK_2}{\sqrt{2\pi r}}\left(\frac{r}{2a}\right)^{i\varepsilon} \tag{3}$$

The normalized SIFs $F_1(\alpha, \beta)$ and $F_2(\alpha, \beta)$ in Eq. (1) varies depending on the material combination and changes in wide ranges as $F_1(\alpha,\beta) = 0\sim\infty, F_2(\alpha,\beta) = 0\sim\infty$. This is because the SIFs are controlled by the intensity of the singular stress field (ISSF) at the interface end without crack. Previously, Noda et al [18-21] have provided the SIF of the small edge interface crack in bi-material bonded strip in the form $F_{1,2}(\alpha, \beta)=C_{1,2}(\alpha, \beta)(W/a)^{1-\lambda}$ by considering the ISSF at the interface end (see Appendix B).

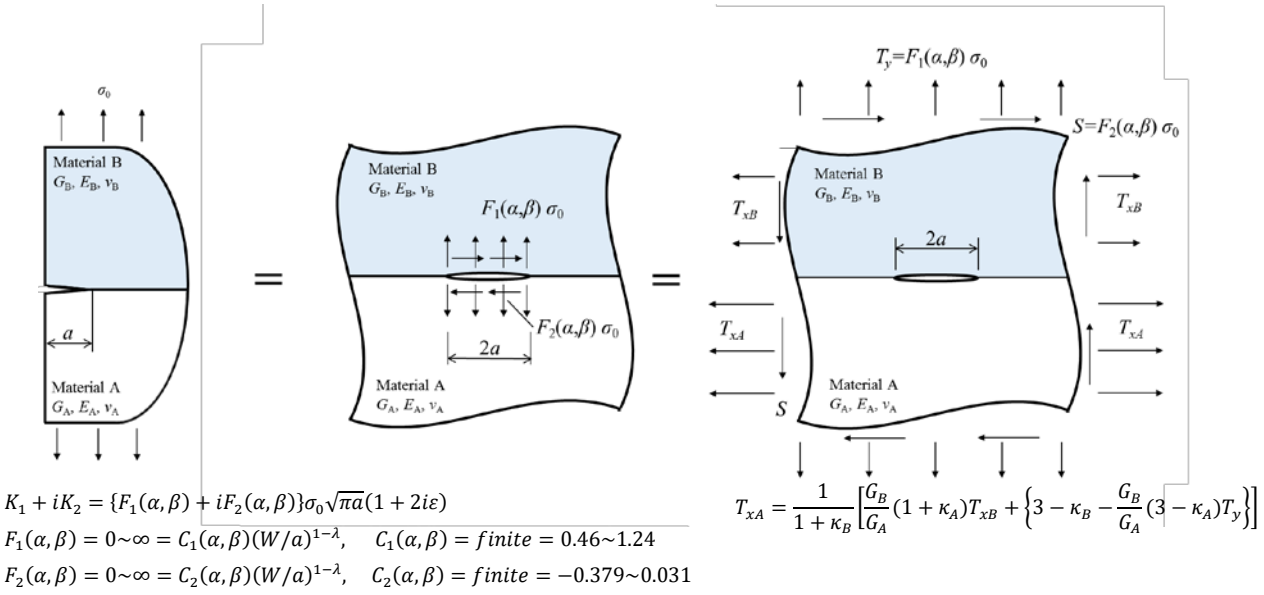

$K_1 + iK_2 = \{F_1(\alpha,\beta) + iF_2(\alpha,\beta)\}\sigma_0\sqrt{\pi a}(1+2i\varepsilon)$

$F_1(\alpha,\beta) = 0\sim\infty = C_1(\alpha,\beta)(W/a)^{1-\lambda}, \quad C_1(\alpha,\beta) = finite = 0.46\sim1.24$

$F_2(\alpha,\beta) = 0\sim\infty = C_2(\alpha,\beta)(W/a)^{1-\lambda}, \quad C_2(\alpha,\beta) = finite = -0.379\sim0.031$

$$T_{xA} = \frac{1}{1+\kappa_B}\left[\frac{G_B}{G_A}(1+\kappa_A)T_{xB} + \left\{3-\kappa_B - \frac{G_B}{G_A}(3-\kappa_A)T_y\right\}\right]$$

(a) (b) (c)

Fig. 3 Eauivalent problems: (a) an edge interface crack whose length is 'a', (b) an interface crack subjected to the normal and tangential tractions along the crack surface, and (c) an interface crack subjected to specified tensile stresses in the x- and y-directions.

2.2 How to Separate Double Singular Stress Fields by Using Stress Value at the Crack Tip without Crack

Figure 4 illustrates a fundamental idea how to separate double singular stress fields. In Fig.4, the most fundamental stress concentration is taken into account by considering an elliptical hole. In other words, the singular stress field due to the interface end in Fig.1 is replaced by the fundamental stress concentration field due to the elliptical hole whose shape ratio is b/c. In Fig.4, therefore, the crack emanating from a semi-elliptical notch is corresponding to the edge interface crack emanating from the interface end in Fig.1.

As shown in Fig.4, the normalized stress intensity factor is defined by using the stress values $\sigma_y(a)$ at the crack tip position. Since the crack tip stress is only one numerical value and not the stress distribution along the whole crack length,

one may think why the crack tip stress is useful. The stress intensity factor (SIF) in Fig.4(a) is equal to the SIF in Fig.4(c), since the SIF in Fig.4(b) is zero. The SIF in Fig.4(c) is approximated by the SIF in Fig.4(c)' and finally the SIF in Fig.4(c). Therefore, the crack tip stress $\sigma_y(a)$ expresses the magnitude of the uniform traction along the crack surface.

Table 1 shows the stress intensity factors of the crack emanating from the elliptical hole in Fig.4. Since Table 1 shows that all values of the normalized SIF are nearly the same, they can be used very conveniently. This is because in Table 1 the stress value $\sigma_y(a)$ at the crack tip position is introduced when there is no crack [22]. Since the stress value $\sigma_y(a)$ is already reflecting the elliptical hole's stress concentration, $F_I=K_I/\sigma_y(a)\sqrt{\pi a}$ is insensitive to the notch shape *b/c* as well as the x-coordinate as shown in Table 1. This is because the effect of the stress concentration due to the notch has been already eliminated. It should be noted that in Table 1 the crack tip stress $\sigma_y(a)/\sigma$ varies in a wide range depending on *a*/ρ and b/c but $F_I=K_I/\sigma_y(a)\sqrt{\pi a}$ is almost constant as F_I=1.12 for 0< *a*/ρ <0.1 and $F_I \to 1.1215$ as $a/\rho \to 0$.

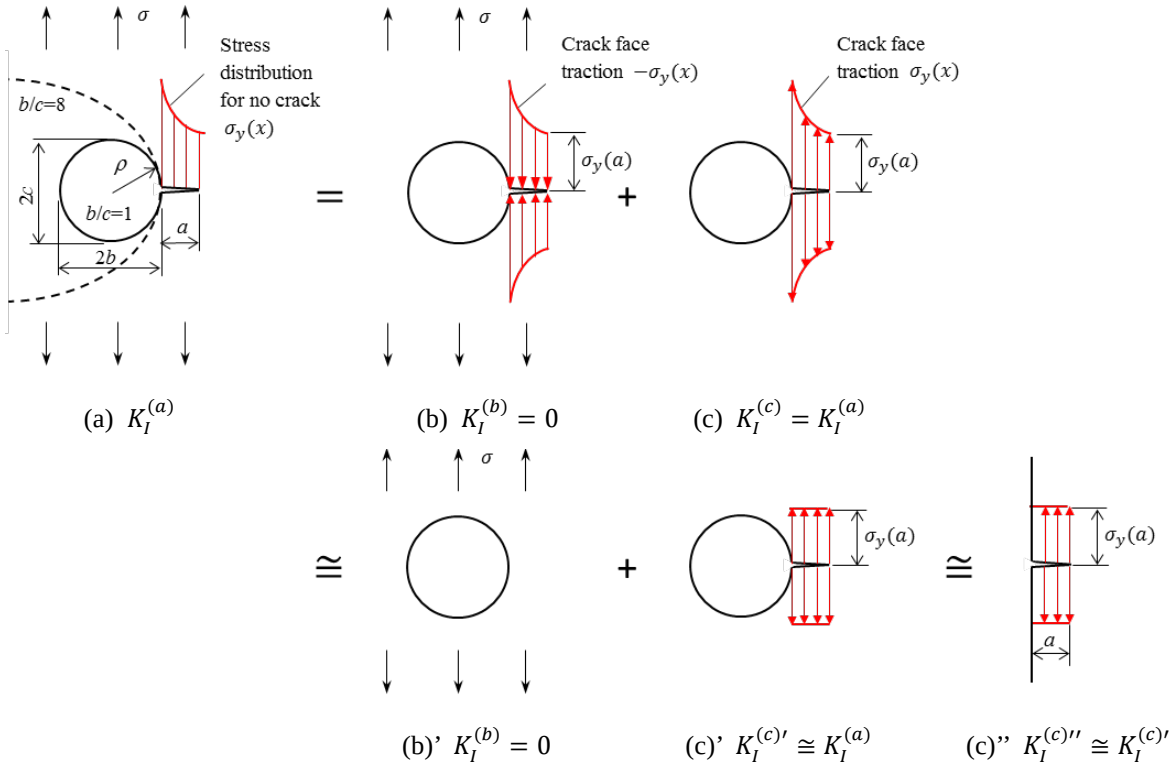

Fig.4 Equivalent crack problems: The stress intensity factor (SIF) in (a) is exactly equal to the SIF in (c) independent of a/ρ. The SIF in (a) is equal to the SIF in (c)' and in (c)'' when $a/\rho \to 0$. Here, $\sigma_y(x)$ is the stress distribution due to the elliptical hole before appearing the crack and $\sigma_y(a)$ is the stress value at the crack tip position [22].

Table 1 Normalized SIF of the crack emanating from an elliptical hole in Fig.4(a)

$F_I = K_I/\sigma_y(a)\sqrt{\pi a}$					
a/ρ	$\to$ 0	0.05	0.1	0.2	0.3
b/c=1	1.122	1.130	1.137	1.147	1.149
b/c=8	1.122	1.126	1.132	1.147	1.162
$\sigma_y(a)/\sigma$					
a/ρ	$\to$ 0	0.05	0.1	0.2	0.3
b/c=1	3.000	2.688	2.438	2.071	1.821
b/c=8	17.00	15.43	14.15	12.20	10.77

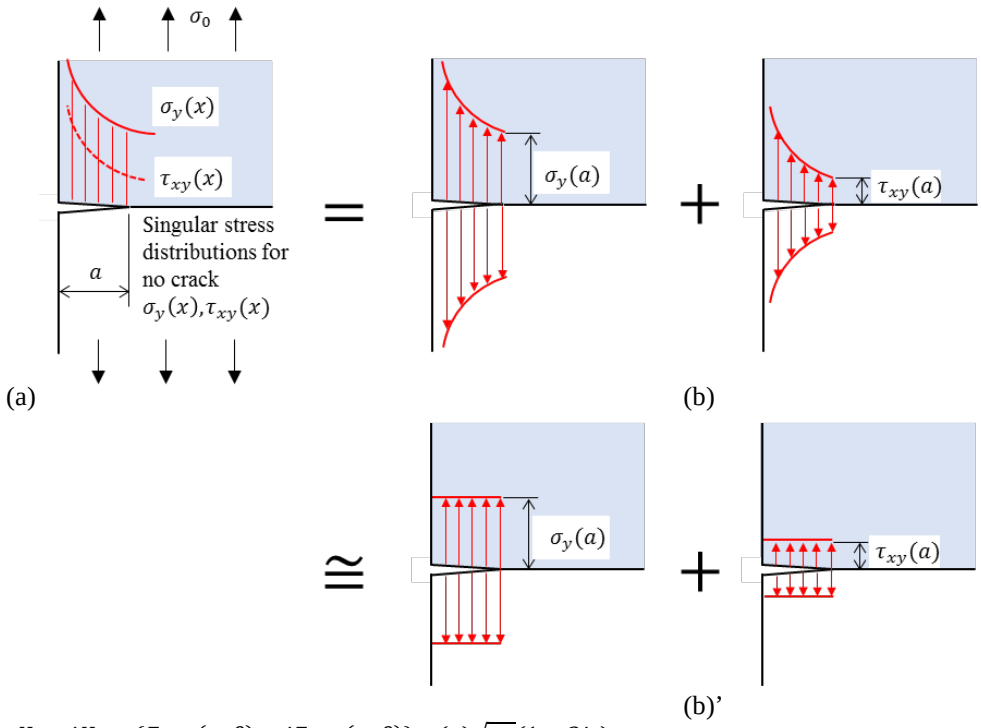

$$K_1 + iK_2 = \{F_{1,int}(\alpha,\beta) + iF_{2,int}(\alpha,\beta)\}\sigma_y(a)\sqrt{\pi a}(1+2i\varepsilon)$$
$$F_1(\alpha,\beta) = finite = 0.808\sim1.50,\ \ F_2(\alpha,\beta) = finite = -0.208\sim0.448$$

Fig. 5 Normalized stress intensity factor (SIF) defined by using the stress values $\sigma_y(a)$ at the crack tip position (see Fig.6 and Table 2). The red line expresses the stress distribution near the interface end without the crack. The SIF in (a) is exactly equal to the SIF in (b). The SIF in (a) is equal to the SIF in (b)' when $a/W \to 0$.

Let's go back to the double singular stress fields in Fig.1. Figure 1(b) illustrates the singular stress filed $\sigma_y(r)$ at the interface end for the bonded AB plate when there is no crack. In this case, the stress $\sigma_y(r) \to \infty$ as $r \to 0$. At the crack tip position $r=a$, therefore, the crack tip stress $\sigma_y(a) \to \infty$ as $a \to 0$ when there is no crack. Therefore, the stress intensity factor of the small edge interface crack whose length is "a" is strongly affected by the singular stress field and the crack tip stress $\sigma_y(a)$ when there is no crack. The singular stress field in bi-material strip was derived in closed form by Chen and Nisitani [23] as shown in Eqs. (4), (5). The singular stress field is controlled by the ISSF (Intensity of Singular Stress Field denoted by K_σ). The singular stress distribution along the interface can be written as

$$\sigma_y(r) = \frac{K_\sigma}{r^{1-\lambda}},\ \ \tau_{xy}(r) = \frac{f_{r\theta}}{f_{\theta\theta}}\frac{K_\sigma}{r^{1-\lambda}} \tag{4}$$

$$f_{\theta\theta} = 2\lambda(\lambda+1)Y_2\sin\left(\frac{\lambda\pi}{2}\right) + 2\lambda^2 Y_1\cos\left(\frac{\lambda\pi}{2}\right),\quad f_{r\theta} = 2\lambda(\lambda-1)Y_1\sin\left(\frac{\lambda\pi}{2}\right) - 2\lambda^2 Y_2\cos\left(\frac{\lambda\pi}{2}\right),$$
$$Y_1 = 4\lambda\beta\cos(\lambda\pi) + 2\beta[\cos(\lambda\pi)-1] + 4\lambda(\lambda+1)(\alpha-\beta),\quad Y_2 = 2(2\lambda\beta-1)\sin(\lambda\pi) \tag{5}$$

In Eqs. (4) and (5), K_σ denotes the ISSF controlling the singular interface stress field. Notations $f_{\theta\theta}$ and $f_{r\theta}$ denote the angular functions where the interface position $\theta = \pi/2$ is inserted. The singular index λ can be determined by solving the eigenequation (6) ,

$$\left[\sin^2\left(\frac{\pi}{2}\lambda\right) - \lambda^2\right]^2\beta^2 + 2\lambda^2\left[\sin^2\left(\frac{\pi}{2}\lambda\right) - \lambda^2\right]\alpha\beta + \lambda^2(\lambda^2-1)\alpha^2 + \frac{\sin^2(\lambda\pi)}{4} = 0 \tag{6}$$

When there is no crack in Fig.1(b), interface stresses $\sigma_y(r)$ and $\tau_{xy}(r)$ are controlled by the ISSF K_σ alone as shown in Eq. (4). In other words, the ratio $\sigma_y(r)/\tau_{xy}(r)=f_{\theta\theta}/f_{r\theta}$ =constant as shown in Eq. (4) because they can be expressed by only the material combination as shown in Eq. (5). Since in Table 1 the SIF K_I in Fig.4 is controlled by $\sigma_y(a)$ independent of the

stress distribution, the SIFs K_1, K_2 of the interface crack in Fig.5 are also controlled by $\sigma_y(a)$ and $\tau_{xy}(a)$ independent of the singular stress distribution. Because of the ratio $\sigma_y(a)/\tau_{xy}(a)$=constant, the SIFs K_1, K_2 are controlled by $\sigma_y(a)$ alone. Therefore, the SIFs of an interface edge crack can be expressed efficiently by using $\sigma_y(a)$ controlled by the ISSF K_σ.

$$K_1 + iK_2 = \{F_{1,int}(\alpha,\beta) + iF_{2,int}(\alpha,\beta)\}\sigma_y(a)\sqrt{\pi a}(1+2i\varepsilon) \tag{7}$$

In Eq. (7), $F_{1,int}(\alpha, \beta)$ and $F_{2,int}(\alpha, \beta)$ are newly defined SIF for interface crack normalized by $\sigma_y(a)$. Although both $\sigma_y(a)$ and $\tau_{xy}(a)$ appear near the interface end, the ratio $\sigma_y(a)/\tau_{xy}(a)$ is constant near the interface end. Hence, only $\sigma_y(a)$ can be used as shown in Eq. (7).

In the previous study [18-21], the interface crack solution defined in Eq. (1) was proposed by using the expression $C_{1,2}(\alpha,\beta) = K_{1,2}/\{(a/W)^{1-\lambda}\sigma_0\sqrt{\pi a}\}$ with Eq. (3). However, this expression includes the plate width W and the singular index λ to show the stress intensity factors K_1, K_2 in Eq. (3). On the other hand, the new definition (7) only includes the singular stress at the crack tip $\sigma_y(a)$.

The advantage of this present solution can be explained in the following way

(1) The new expression does not include singularity index λ of the corner singular stress field when there is no crack

(2) The new expression include the crack tip stress value σ_y (a) instead when there is no crack. However, this value σ_y (a) can be determined easily and accurately by using the standard finite element method.

(3) The new expression can be applied to other geometries. For example, it can be applied to the edge interface crack situated at the butt joint as shown in Fig.1 (c). This is because the effect of other geometry can be reflected by σ_y (a).

One may think that the new definition (7) only considers the singular stress at the crack tip and does not includes the plate width W, therefore, it is not suitable for the finite width plate problem. However, the dimensionless SIFs proposed in this study are based on the crack tip stress $\sigma_y(a)$. Since the singular stress field at the interface end in bi-material and butt joint without the crack is affected by the plate width W, the effect of a/W is included in $\sigma_y(a)$. Therefore the present solution is useful for the problem of the finite plate.

3. New stress intensity factor solution for edge interface crack based on the crack tip stress when there is no crack

By applying the proportional method, the stress intensity factors in Fig.1(a) can be obtained systematically. Figure 6 shows the SIFs $F_{1,int}(\alpha, \beta)$ and $F_{2,int}(\alpha, \beta)$ normalized by the crack tip stress $\sigma_y(a)$ for the whole range of material combination. Tables 2(a), (b) show the normalized SIF values when α>0 on Dundurs' parameters. The free-edge singularity in Fig.1(b) depends on the material combination. The singularity index λ<1 (bad pair) when $\alpha(\alpha-2\beta)$>0; λ>1 (good pair) when $\alpha(\alpha-2\beta)$<0; and λ=1 (equal pair) when $\alpha(\alpha-2\beta)$=0 [9]. In Table 2, red figures indicate bad pair, blue figures indicate good pair and black figures indicate equal pair. Since Table 2 and Fig.6 show the results over the entire range of α - β, they can be applied to any material combinations.

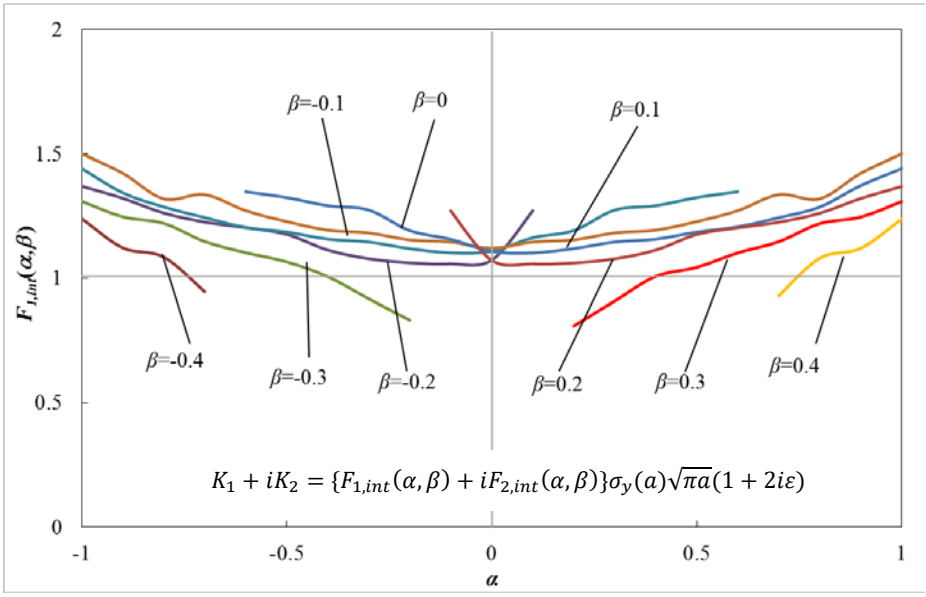

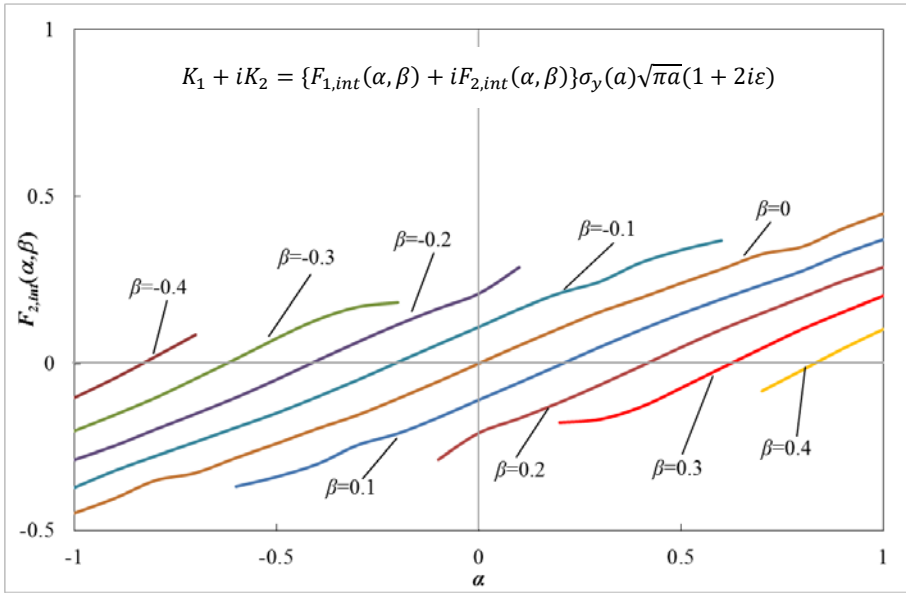

Fig.6 Values of $F_{1,int}(\alpha, \beta)$ and $F_{2,int}(\alpha, \beta)$ as a function of α and β.

Table 2(a) Values of $F_{1,\mathrm{int}}$ as a function of α and β $[K_1 + iK_2 = \{F_{1,int}(\alpha,\beta) + iF_{2,int}(\alpha,\beta)\}\sigma_y(a)\sqrt{\pi a}(1+2i\varepsilon)]$.

[Red figures indicate bad pair α(α−2β)>0, blue figures indicate good pair α(α−2β)<0, black figures indicate equal pair α(α−2β)=0]

α	β=-0.2	β=-0.1	β=0	β=0.1	β=0.2	β=0.3	β=0.4
0	1.073	1.109	1.121	1.108	1.072		
0.1	1.271	1.163	1.146	1.102	1.058		
0.2		1.192	1.154	1.119	1.061	0.808	
0.3		1.274	1.182	1.146	1.078	0.909	
0.4		1.292	1.194	1.157	1.113	1.008	
0.5		1.325	1.228	1.186	1.176	1.044	
0.6		1.348	1.272	1.207	1.203	1.102	
0.7			1.337	1.244	1.226	1.147	0.929
0.8			1.320	1.287	1.262	1.220	1.081
0.9			1.423	1.373	1.321	1.246	1.121
1.0			1.500	1.441	1.369	1.309	1.238

Table 2(b) Values of $F_{2,\mathrm{int}}$ as a function of α and β $[K_1 + iK_2 = \{F_{1,int}(\alpha,\beta) + iF_{2,int}(\alpha,\beta)\}\sigma_y(a)\sqrt{\pi a}(1+2i\varepsilon)]$.

[Red figures indicate bad pair α(α−2β)>0, blue figures indicate good pair α(α−2β)<0, black figures indicate equal pair α(α−2β)=0]

α	β=-0.2	β=-0.1	β=0	β=0.1	β=0.2	β=0.3	β=0.4
0	0.209	0.109	0.000	-0.109	-0.208		
0.1	0.288	0.163	0.054	-0.057	-0.165		
0.2		0.210	0.105	-0.004	-0.117	-0.177	
0.3		0.245	0.155	0.050	-0.064	-0.167	
0.4		0.301	0.196	0.101	-0.009	-0.131	
0.5		0.339	0.240	0.149	0.048	-0.075	
0.6		0.368	0.282	0.192	0.102	-0.014	
0.7			0.327	0.235	0.151	0.046	-0.083
0.8			0.349	0.277	0.198	0.103	-0.019
0.9			0.404	0.328	0.246	0.154	0.045
1.0			0.448	0.371	0.288	0.202	0.103

4. Usefulness of new stress intensity factor solution by applying to ABC sandwiched plate

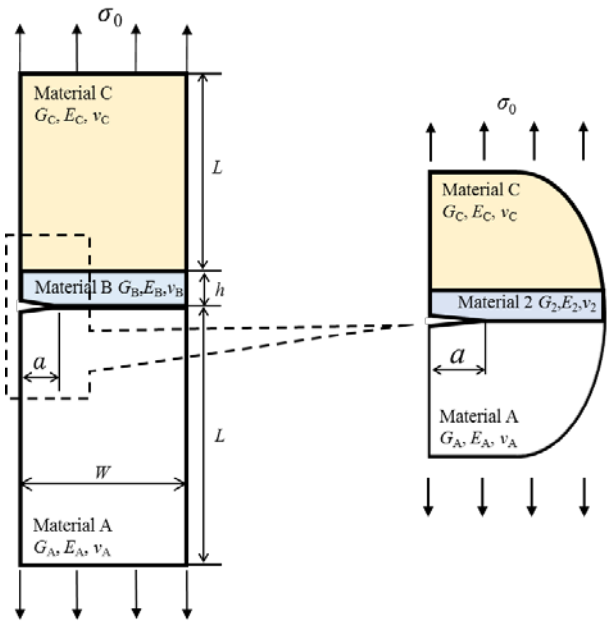

Fig. 7 ABC sandwiched butt joints with an interface edge crack subjected to tension.

Table 3 Material properties used in the present analyses.

Group	Material A (lower)		Material B (adhesion layer)		Material C (upper)		Edge singularity	
	E_A[GPa]	ν_A	E_B[GPa]	ν_B	E_C[GPa]	ν_C	Interface AB	Interface BC
1	1000.0	0.002	176.471	0.118	70.3	0.345	Bad pair	Bad pair
2	1000.0	0.002	176.471	0.118	238.3	0.35	Bad pair	Good pair
3	1000.0	0.409	333.333	0.003	15.34	0.15	Good pair	Bad pair
4	1000.0	0.409	333.333	0.003	466	0.26	Good pair	Good pair

Table 4 Dundurs' parameters and the singularity index for material combination shown in Table 3.

Group	α_{AB}	β_{AB}	α_{BC}	β_{BC}	$1-\lambda_{AB}$	$1-\lambda_{BC}$	$F_1(\alpha,\beta)$	$F_2(\alpha,\beta)$
1	0.7	0.3	-0.430	-0.109	0.0652	0.0679	1.147	0.046
2	0.7	0.3	0.149	0.115	0.0652	-0.0102	1.147	0.046
3	0.5	0.3	0.912	-0.384	-0.0558	0.1317	1.044	-0.075
4	0.5	0.3	0.167	0.134	-0.0558	-0.0151	1.044	-0.075

To confirm the usefulness of the present solution, the analysis is performed for the edge interface crack in ABC sandwiched butt joint shown in Fig.7. The interface crack with length '*a*' is assumed along the interface AB. Here, interface AB means the interface between the materials A and B. In this analysis, the effect of the different material C on the stress intensity factor of edge interface crack as well as the effect of the bond line thickness is considered. The butt joint FEM model is made by using 8 nodes quadrilateral elements. The remote tensile stress σ_0=1 MPa and the interface crack length a=1 mm are assumed. A very refined mesh pattern is used to obtain the accurate stress value at the crack tip position, the smallest element size e near the crack tip is $e/a=1/3^6$.

As shown in Table 3 and Table 4, four patterns of material combinations are selected from Group 1 to Group 4, which have different singularities at interface AB and interface BC. The details of material properties, Dundurs' parameters and edge singularity indexes are indicated in Table 3 and Table 4.

Figure 8 (a), (b) and Table 5 show the effect of crack length a/h on the normalized SIF $F_{1,\mathrm{int}}(\alpha, \beta)$ and $F_{2,\mathrm{int}}(\alpha, \beta)$ defined in Eq. (7) in ABC sandwiched butt joint subjected to tension. FEM analysis is performed for Group1 ~ 4 in Table 3 and Table 4 under the fixed bond line thickness h/W=0.01. In Fig. 8, constant values are obtained when a/h<0.01 in the new definition (7) of the SIFs $F_{1,\mathrm{int}}(\alpha, \beta)$ and $F_{2,\mathrm{int}}(\alpha, \beta)$ for Group 1 ~ 4 in Table 3 under fixed bond line thickness h/W=0.01. When a/h<0.01, the dimensionless factors $F_{1,\mathrm{int}}(\alpha, \beta)$ and $F_{2,\mathrm{int}}(\alpha, \beta)$ coincide with the results in Table 2 under the same α_{AB} and β_{AB} . Therefore, the normalized factors $F_{1,\mathrm{int}}(\alpha, \beta)$ and $F_{2,\mathrm{int}}(\alpha, \beta)$ can be determined by the material combination A and B when the relative crack length a/h<0.01.

Figure 9 (a), (b) and Table 6 show the effect of the bond line thickness h/W on the normalized SIFs $F_{1,\mathrm{int}}(\alpha, \beta)$ and $F_{2,\mathrm{int}}(\alpha, \beta)$ defined in Eq. (7). FEM analysis is performed by varying the bond line thickness in the range 0.002 <h/W<1.0 under the fixed crack length $a/W=10^{-6}$. In Fig.9, the parenthesis value shows the ISSF K_σ when there is no crack. The ISSF K_σ varies depending on the bond line thickness although the values of normalized SIFs stay approximately constant in the wide range of h/W. As shown in Fig.9, constant values are obtained independent of h/W in the new definition (7) of the SIF F_1, F_2 for Group 1~Group 4 in Table 3 under fixed crack length $a/W=10^{-6}$, that is, $a/h<10^{-2}$ although the ISSF K_σ parenthesis varies widely. In Fig.9, the results of $a/W=10^{-6}$ are indicated. One may think that the present solution can be applied to only very small crack like $a/W=10^{-6}$. However, Fig.8 shows that the present solution is useful in the range a/h<0.1 less than 6 percent error as well as in the range a/h<0.01 less than 1 percent error. Fig.9 shows the case of $h/W=10^{-3}$ ~ 1. It should be noted that since $h<W$, a/h should be considered to discuss the application range of the present solution. The dimensionless SIFs defined in this study are based on the crack tip stress $\sigma_y(a)$. Since the intensity of singular stress field (ISSF) K_σ at the interface end is affected by the plate width W, the effect of a/W is included in σy (a). Therefore, the present solution is useful for the problem of the finite plate.

From above numerical results, we concluded that the normalized SIFs of small edge interface crack defined by Eq.(7) are related only to Dundurs' parameter of materials A and B independent of the material C, bond line thickness and plate length when the crack length a/W<0.01 and a/h<0.01.

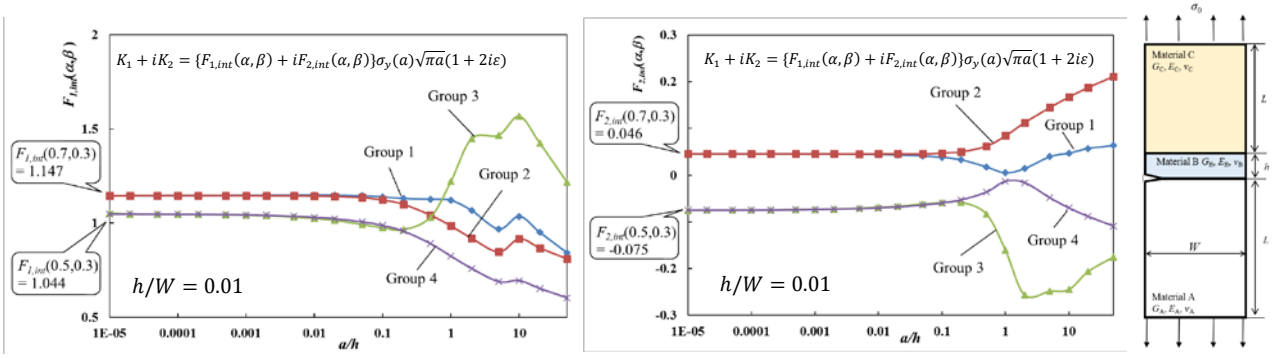

(a) $F_{1,\mathrm{int}}(\alpha,\beta)$ vs. a/h (b) $F_{2,\mathrm{int}}(\alpha,\beta)$ vs. a/h

Fig. 8 Constant values are obtained when a/h<0.01 in the new definition (7) of the SIF F_1, F_2 for Group 1~Group 4 in Table 3 under fixed bond line thickness h/W=0.01. (a) $F_{1,\mathrm{int}}(\alpha,\beta)$ vs. a/h (b) $F_{2,\mathrm{int}}(\alpha,\beta)$ vs. a/h

Table 5 Values of the new definition of SIF for Group 1 – Group 4 under fixed bond line thickness h/W=0.01.

a/h	$F_{1,\mathrm{int}}(0.7,0.3)$		$F_{1,\mathrm{int}}(0.5,0.3)$		$F_{2,\mathrm{int}}(0.7,0.3)$		$F_{2,\mathrm{int}}(0.5,0.3)$	
	Group 1	Group 2	Group 3	Group 4	Group1	Group 2	Group 3	Group 4
10	1.036	0.917	1.567	0.695	0.0471	0.1670	-0.2447	-0.0701
1	1.121	0.985	1.223	0.825	0.0050	0.0840	-0.1609	-0.0131
0.1	1.140	1.123	0.976	0.988	0.0381	0.0473	-0.0587	-0.0595

0.01	1.149	1.145	1.035	1.034	0.0442	0.0454	-0.0688	-0.0701
0.001	1.148	1.147	1.042	1.044	0.0454	0.0455	-0.0731	-0.0736
0.0001	1.147	1.147	1.047	1.044	0.0455	0.0455	-0.0745	-0.0746
0.00001	1.147	1.147	1.044	1.044	0.0455	0.0455	-0.0753	-0.0750

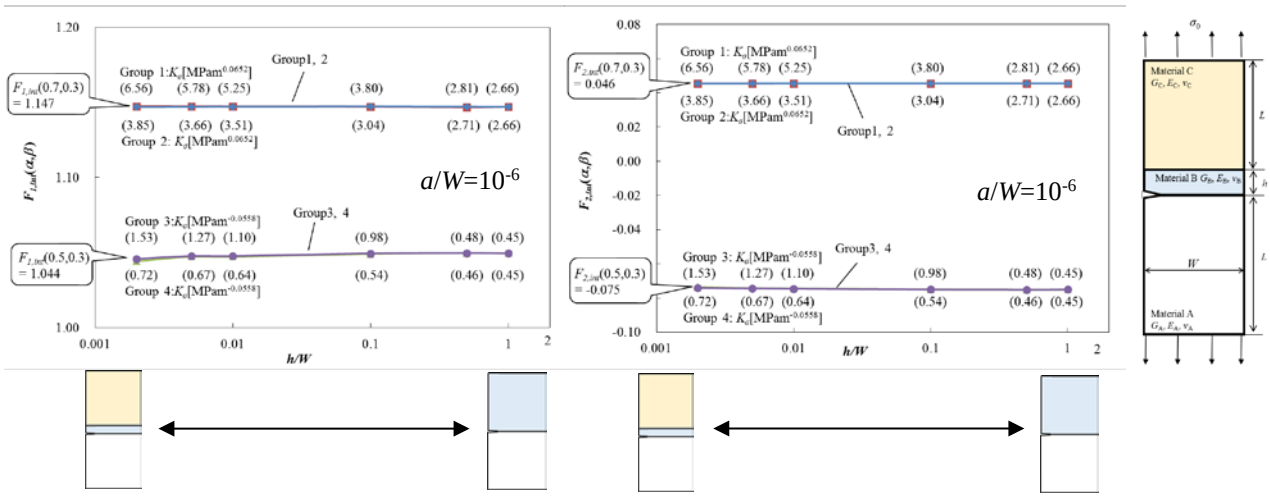

(a) $F_{1,\mathrm{int}}(\alpha,\beta)$ vs. h/W (b) $F_{2,\mathrm{int}}(\alpha,\beta)$ vs. h/W

Fig.9 Constant values are obtained independent of h/W in the new definition (7) of the SIFs $F_{1,\mathrm{int}}(\alpha,\beta)$, $F_{2,\mathrm{int}}(\alpha,\beta)$ for Group 1~Group 4 in Table 3 under fixed crack length $a/W=10^{-6}$, although the ISSF K_σ parenthesis varies widely. (a) $F_{1,int}(\alpha,\beta)$ vs. h/W (b) $F_{2,int}(\alpha,\beta)$ vs. h/W

Table 6 Values of the new definition of SIFs $F_{1,\mathrm{int}}(\alpha,\beta)$, $F_{2,\mathrm{int}}(\alpha,\beta)$ for Group 1 – Group 4 under fixed crack length $a/W=10^{-6}$.

h/W	$F_{1,\mathrm{int}}(0.7,0.3)$		$F_{1,\mathrm{int}}(0.5,0.3)$		$F_{2,\mathrm{int}}(0.7,0.3)$		$F_{2,\mathrm{int}}(0.5,0.3)$	
	Group 1	Group 2	Group 3	Group 4	Group1	Group 2	Group 3	Group 4
1	1.147	1.147	1.050	1.049	0.046	0.046	-0.075	-0.075
0.5	1.147	1.147	1.050	1.050	0.046	0.046	-0.075	-0.075
0.1	1.147	1.147	1.049	1.049	0.046	0.046	-0.075	-0.075
0.01	1.147	1.147	1.047	1.048	0.046	0.046	-0.074	-0.075
0.005	1.147	1.147	1.047	1.048	0.045	0.045	-0.074	-0.074
0.002	1.148	1.147	1.044	1.046	0.045	0.045	-0.074	-0.074

5. Conclusion

In this study, the stress intensity factor solution of the interface edge crack in a bonded plate was examined. The stress intensity factor of the interface crack is strongly affected by the singular stress field at the interface edge without crack. To separate double singular stress fields, the expression of the stress intensity factors K_1 and K_2 was investigated by using the singular stress $\sigma_y(a)$ at the crack tip point without the crack. The conclusions are summarized as follows.

(1) The new stress intensity factor solution for edge interface crack in bi-material plate was presented. The stress intensity factor of the edge interface crack can be expressed as

$$K_1 + iK_2 = \{F_{1,int}(\alpha,\beta) + iF_{2,int}(\alpha,\beta)\}\sigma_y(a)\sqrt{\pi a}(1+2i\varepsilon), \varepsilon = \frac{1}{2\pi}\ln\left[\left(\frac{\kappa_A}{G_A}+\frac{1}{G_B}\right)\Big/\left(\frac{\kappa_B}{G_B}+\frac{1}{G_A}\right)\right]$$

The crack tips stress σ_y (a) can be determined easily and accurately by using the standard finite element method.

(2) The normalized factors $F_1(\alpha,\beta)$ and $F_2(\alpha,\beta)$ in the whole range of material combination expressed by Dundurs' parameters were presented in Fig.6 and tabulated in Table 2. By using these factors, it is possible to evaluate the stress intensity factors of the small interface crack for any material combination.

(3) To confirm the usefulness of the present solution, the edge interface crack in ABC sandwiched butt joint was analyzed. FEM analysis was performed by varying the crack length, the bond line thickness and the material combination. It was found that the normalized SIFs $F_{1,\mathrm{int}}(\alpha, \beta)$ and $F_{2,\mathrm{int}}(\alpha, \beta)$ of small edge interface crack defined by Eq.(7) relate only to Dundurs' parameter of materials A and B, regardless of the material C and the bond line thickness when the crack length a/W<0.01 and a/h<0.01.

References

[1] Charalambides, P. G., Lund, J., Evans, A. G., McMeeking, R. M., A Test Specimen for Determining the Fracture Resistance of Bimaterial Interfaces, Transaction of ASME Series E, Journal of Applied Mechanics, Vol.56, Issue 1, (1989) pp.77-82.

[2] O'Dowd, N.P., Shih, C.F., Stout, M.G., Test geometries for measuring interfacial fracture toughness, International Journal of Solids and Structures, Vol. 29, No.5, (1992), pp. 571-589.

[3] Yuuki, R., Liu, J.-Q., Xu, J.-Q., Ohira, T., Ono, T., Mixed mode fracture criteria for an interface crack, Engineering Fracture Mechanics, Vol. 47, No. 3, (1994), pp. 367-377.

[4] Xu, L., Tippur, H.V., Fracture parameters for interfacial cracks: an experimental-finite element study of crack tip fields and crack initiation toughness, International Journal of Fracture, Vol. 71, (1995), pp. 345-363.

[5] Ikeda, T., Miyazaki, N., Soda, T., Mixed mode fracture criterion of interface crack between dissimilar materials, Engineering Fracture Mechanics, Vol. 59, No. 6, (1998), pp. 725-735.

[6] Afendi M., Teramoto T., Fracture toughness test of epoxy adhesive dissimilar joint with various adhesive thicknesses, Journal of Solid Mechanics and Materials Engineering, Vol.4, No.7 (2010), pp.999-1010.

[7] Akisanya A.R., Fleck N.A., Interfacial cracking from the free-edge of long bi-material strip, International Journal of Solids and Structures, Vol. 34, No.13 (1997), pp.1645-1665.

[8] Ioka S., Matsuda T., Kubo S., A numerical and theoretical study on relationship between stress intensity factor of a small interface crack on interface and free-edge stress singularity of bonded dissimilar materials, Journal of the Society of Materials Science, Japan, Vol. 51, No. 12 (2002), pp. 1373-1379 (in Japanese).

[9] Zhang, Y., Noda, N.-A., Wu, P. and Duan, M., A mesh-independent technique to evaluate stress singularities in adhesive joints, International Journal of Adhesion & Adhesives, Vol. 57 (2015), pp. 105-117. [No.60 (2015), pp.130]

[10] Noda N.-A., Uchikoba T., Ueno M., Sano Y., Iida K., Wang Z., Wang G., Convenient debonding strength evaluation for spray coating based on intensity of singular stress, ISIJ International, Vol. 55, No.12 (2015), pp. 2624-2630.

[11] Wang, Z., Noda, N.-A., Ueno, M. and Sano, Y., Optimum Design of Ceramic Spray Coating Evaluated in Terms of Intensity of Singular Stress Field, Steel Research International, Vol.88, Issue 7 (2017) doi: 10.1002/srin.201600353

[12] Miyazaki, T., Noda, N.-A., Ren, F., Wang, Z., Sano, Y. and Iida, K., Analysis of intensity of singular stress field for bonded cylinder and bonded pipe in comparison with bonded plate, International Journal of Adhesion & Adhesives, Vol. 77 (2017), pp. 118-137.

[13] Li, R., Noda, N.-A., Takaki, R., Sano, Y., Takase Y., Miyazaki, T., Most suitable evaluation method for adhesive strength to minimize bend effect in lap joints in terms of the intensity of singular stress field, International Journal of Adhesion and Adhesives, Vol. 86 (2018), pp. 45-58.

[14] Noda, N.-A., Miyazaki, T., Uchikoba, T., Li, R., Sano, Y. and Takase, Y., Convenient debonding strength evaluation based on the intensity of singular stress for adhesive joints, Journal of The Japan Institute of Electronics Packaging, Vol. 17, No.2 (2014), pp. 132-142 (in Japanese).

[15] Noda, N.-A., Miyazaki, T., Li, R., Uchikoba, T., Sano, Y. and Takase, Y., Debonding strength evaluation in terms of

the intensity of singular stress at the interface corner with and without fictitious crack, International Journal of Adhesion and Adhesives, Vol. 61 (2015), pp. 46-64.

[16] Oda, K., Kamisugi, K. and Noda, N.-A., Analysis of stress intensity factor for interface cracks based on proportional method, Transactions of the Japan Society of Mechanical Engineers, Series A, Vol. 75, No. 752 (2009), pp. 476-482 (in Japanese).

[17] Kakuno, H., Oda, K., Morisaki, T., Analysis of stress intensity factor for interfacial crack in bonded dissimilar plate under bending, Key Engineering Materials, Vols. 417-418 (2010), pp. 153-156.

[18] Noda, N.-A., Lan, X., Michinaka, K., Zhang, Y., Oda, K., Stress intensity factor of an edge interface crack in a bonded semi-infinite plate, Transactions of the Japan Society of Mechanical Engineers, Series A, Vol. 76, No. 770 (2010), pp. 1270-1277 (in Japanese).

[19] Lan, X., Noda, N.-A., Mithinaka, K., Zhang, Y., The effect of material combinations and relative crack size to the stress intensity factors at the crack tip of a bi-material bonded strip, Engineering Fracture Mechanics, Vol. 78 (2011), pp. 2572-2584.

[20] Oda, K., Lan, X., Noda, N.-A. and Michinaka, K., Effect of arbitrary bi-material combination and bending loading conditions on stress intensity factors of an edge interface crack, International Journal of Structural Integrity, Vol.3, No.4 (2012-11), pp.457-475.

[21] Noda, N.-A., Lan, X., Stress intensity factors for an edge interface crack in a bonded semi-infinite plate for arbitrary material combination, International Journal of Solids and Structures, Vol.49 (2012), pp. 1241–1251.

[22] Nisitani H., Chen D.H., Isida M., An approximate method for calculating K_I and K_{II} of various edge cracks emanating from the apex of an elliptic hole, Transactions of the Japan Society of Mechanical Engineers, Series A, Vol. 50, No. 451 (1984), pp. 341-350 (in Japanese).

[23] Chen D.H., Nisitani H., Intensity of singular stress field near the interface edge point of a bonded strip, Transactions of the Japan Society of Mechanical Engineers, Series A, Vol. 59, No. 567 (1993), pp. 2682-2686 (in Japanese).

[24] Noda N-A, Chen X, Sano Y, Wahab MA, Maruyama H, Fujisawa R, Takase Y. Effect of pitch difference between the boltnut connections upon the antiloosening performance and fatigue life. Mater Des 2016;96:476–89.

Appendix A. Proportional Method

In this study, the stress intensity factor of interface crack is calculated by the proportional method [16,17]. In the method, stress values at the crack tip node are used and a stress intensity factor is determined by the ratio of the crack tip stress values between an unknown problem and the reference problem as shown in Fig.A1. The method gives the singular stress field equal to the unknown problem by adjusting load stress T_y and S of the reference problem whose the stress intensity factor is already-known. The single interface crack in a bonded semi-infinite plate subjected to the tension T_y and shear S is selected as the reference problem because the interface crack tip is always mixed mode state. The stress values at the interface crack tip node calculated by FEM in the reference problem under the tensile stress T_y=1 (S=0) or shear stress S=1 (T_y=0) are written by $\sigma_{y0,FEM}^{T_y=1\ *}$, $\tau_{xy0,FEM}^{T_y=1\ *}$ and $\sigma_{y0,FEM}^{S=1\ *}$, $\tau_{xy0,FEM}^{S=1\ *}$, respectively. The crack tip stress values of the unknown problem are also denoted by $\sigma_{y0,FEM}$, $\tau_{xy0,FEM}$. By using the same crack tip stress condition between the reference and the unknown problems, that is, $\sigma_{y0,FEM} = \sigma_{y0,FEM}^{*}$ and $\tau_{xy0,FEM} = \tau_{xy0,FEM}^{*}$, the external loading stress T_y and S in the reference problem can be determined from the next expression.

$$T_y = \frac{\sigma_{y0,FEM} \cdot \tau_{xy0,FEM}^{S=1\ *} - \sigma_{y0,FEM}^{S=1\ *} \cdot \tau_{xy0,FEM}}{\sigma_{y0,FEM}^{T_y=1\ *} \cdot \tau_{xy0,FEM}^{S=1\ *} - \sigma_{y0,FEM}^{S=1\ *} \cdot \tau_{xy0,FEM}^{T_y=1\ *}}, \qquad S = \frac{\sigma_{y0,FEM}^{T_y=1\ *} \cdot \tau_{xy0,FEM} - \sigma_{y0,FEM} \cdot \tau_{xy0,FEM}^{T_y=1\ *}}{\sigma_{y0,FEM}^{T_y=1\ *} \cdot \tau_{xy0,FEM}^{S=1\ *} - \sigma_{y0,FEM}^{S=1\ *} \cdot \tau_{xy0,FEM}^{T_y=1\ *}} \tag{A1}$$

From the loading stresses T_y and S obtained by Eq.(A1), the stress intensity factor of the interface crack in the reference problem can be evaluated by

$$K_1^* + iK_2^* = (T_y + iS)\sqrt{\pi a^*}(1 + 2i\varepsilon), \qquad \varepsilon = \frac{1}{2\pi} ln\left[\left(\frac{\kappa_A}{G_A} + \frac{1}{G_B}\right)\Big/\left(\frac{\kappa_B}{G_B} + \frac{1}{G_A}\right)\right] \tag{A2}$$

The definition of stress intensity factor shown in Eq.(A2) is based on the interface crack length $2a^*$.

$$\sigma_y + i\tau_{xy} = \frac{K_1^* + iK_2^*}{\sqrt{2\pi r}}\left(\frac{r}{2a^*}\right)^{i\varepsilon} \tag{A3}$$

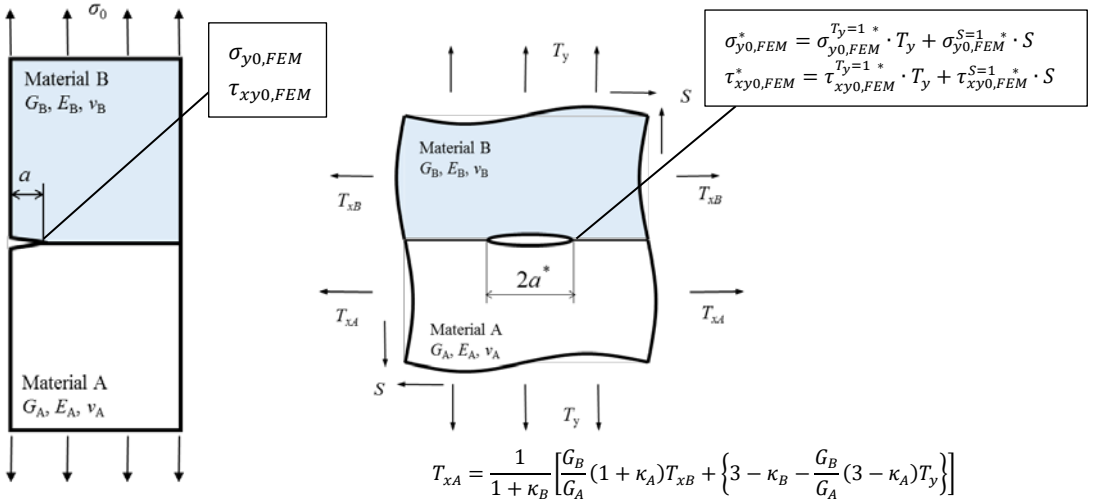

(a) Given problem (b) Reference problem

Fig.A1 Demonstration of (a) the given problem and (b) the reference problem. The proportional method is based on the fact that the crack tip stress values obtained by FEM are controlled by the singular stress field near the interface crack tip.

Here, ε is the oscillation singular index, $\kappa_i = 3 - 4\nu_i$ (plane strain), $(3-\nu_i)/(1+\nu_i)$ (plane stress). Because the stress intensity factor of Eq. (A2) is equal to that of the unknown problem, the stress intensity factors of the unknown problem in Fig. A1(a) can be obtained as

$$K_1 = K_1^*, \quad K_2 = K_2^*. \tag{A4}$$

It is noted that in the proportional method the finite element models of the reference and the unknown problems have the same crack length and the same FEM mesh pattern near the interface crack tip [16, 17].

Appendix B. Previous definition of the edge interface crack in bi-material plate

The one of authors has reported in the previous paper that an edge interface crack in a bonded strip were analyzed with varying the crack length and material combinations systematically [18-21]. Then, the limiting solutions were provided in a bonded dissimilar semi-infinite plate subjected to remote uniform tension under arbitrary material combinations [21].

The stress intensity factors are expressed for an edge crack in bonded semi-infinite plate in the following form

$$\begin{cases} \dfrac{K_1}{\sigma\sqrt{\pi a}}, \dfrac{K_2}{\sigma\sqrt{\pi a}} \to 0 \ \textbf{when} \ \alpha(\alpha - 2\beta) < 0 \ \textbf{(good pair)} \\ \dfrac{K_1}{\sigma\sqrt{\pi a}} = 1.121 + 0.0159\beta - 0.221\beta^2, \dfrac{K_2}{\sigma\sqrt{\pi a}} = -0.684\beta \to 0 \ \textbf{when} \ \alpha(\alpha - 2\beta) = 0 \ \textbf{(equal} \\ \dfrac{K_1}{\sigma\sqrt{\pi a}}, \dfrac{K_2}{\sigma\sqrt{\pi a}} \to \infty \ \textbf{when} \ \alpha(\alpha - 2\beta) > 0 \ \textbf{(bad pair)} \end{cases} \tag{A5}$$

The stress intensity factors for the small interface edge crack in a bonded strip are controlled by the singular stress field at the interface end. It is found that the stress intensity factors can be expressed in following forms if the edge interface crack is small enough within the zone of free-edge singularity of a bonded strip. Those coefficients C_1, C_2 are computed and tabulated under all material combinations in the α-β space.

$$C_1 = \frac{K_1}{\sigma\sqrt{\pi a}}(a/W)^{1-\lambda}, C_2 = \frac{K_2}{\sigma\sqrt{\pi a}}(a/W)^{1-\lambda} \tag{A6}$$

As indicated in Table A1, C_1 and C_2 always have finite values when $a/W \to 0$.

Table A1 Values of C_1 and C_2 in eqn (A6) [21]

Tabulated values of C_1.

α	β = −0.2	β = −0.1	β = 0	β = 0.1	β = 0.2	β = 0.3	β = 0.4	β = 0.45
0.05	1.036	1.082	1.114	1.136				
0.1	0.979	1.043	1.094	1.146	1.187			
0.15	0.907	1.001	1.063	1.14	1.221			
0.2		0.958	1.025	1.12	1.24			
0.3		0.875	0.938	1.044	1.215			
0.4		0.798	0.852	0.947	1.115	1.528		
0.5		0.721	0.772	0.85	0.986	1.343		
0.6			0.7	0.763	0.863	1.106		
0.7			0.635	0.686	0.756	0.912	1.876	
0.75			0.604	0.651	0.709	0.833	1.356	
0.8			0.573	0.618	0.666	0.764	1.092	
0.85			0.542	0.586	0.626	0.704	0.925	1.589
0.9			0.508	0.556	0.588	0.65	0.806	1.083
0.95			0.46	0.527	0.553	0.602	0.715	0.867

Tabulated values of C_2.

α	β = −0.2	β = −0.1	β = 0	β = 0.1	β = 0.2	β = 0.3	β = 0.4	β = 0.45
0.05	−0.083	−0.06	−0.026	0.014				
0.1	−0.093	−0.079	−0.052	−0.013	0.031			
0.15	−0.098	−0.094	−0.074	−0.041	0.006			
0.2		−0.106	−0.094	−0.067	−0.023			
0.3		−0.124	−0.123	−0.113	−0.084			
0.4		−0.133	−0.141	−0.144	−0.135	−0.095		
0.5		−0.137	−0.151	−0.162	−0.169	−0.166		
0.6			−0.156	−0.172	−0.187	−0.204		
0.7			−0.156	−0.176	−0.194	−0.218	−0.318	
0.75			−0.155	−0.176	−0.195	−0.219	−0.288	
0.8			−0.153	−0.175	−0.194	−0.219	−0.273	
0.85			−0.15	−0.173	−0.193	−0.217	−0.262	−0.379
0.9			−0.145	−0.171	−0.19	−0.214	−0.252	−0.307
0.95			−0.136	−0.168	−0.187	−0.209	−0.243	−0.278